A distinct subset of FcγRI-expressing Th1 cells exert antibody-mediated cytotoxic activity

Diana Rasoulouniriana,[1] Nadine Santana-Magal,[1] Amit Gutwillig,[1] Leen Farhat-Younis,[1] Yariv Wine,[2] Corey Saperia,[1] Lior Tal,[1] Haim Gutman,[3,4] Alexander Tsivian,[4] Ronen Brenner,[4,5] Eiman Abu Bandora,[1] Nathan E. Reticker-Flynn,[6] Peleg Rider,[1] and Yaron Carmi[1]

[1]Department of Pathology, [2]Department of Biotechnology, and [3]Department of Surgery, Sackler School of Medicine, Tel Aviv University, Tel Aviv, Israel. [4]Surgical Oncology Unit, Rabin Medical Center, Beilinson Campus, Petach Tikva, Israel. [5]Wolfson Medical Center, Holon, Israel. [6]Department of Pathology, Stanford School of Medicine, Stanford, California, USA.

While a high frequency of Th1 cells in tumors is associated with improved cancer prognosis, this benefit has been attributed mainly to support of cytotoxic activity of CD8⁺ T cells. By attempting to potentiate antibody-driven immunity, we found a remarkable synergy between CD4⁺ T cells and tumor-binding antibodies. This surprising synergy was mediated by a small subset of tumor-infiltrating CD4⁺ T cells that express the high-affinity Fcγ receptor for IgG (FcγRI) in both mouse and human patients. These cells efficiently lyse tumor cells coated with antibodies through concomitant crosslinking of their T cell receptor (TCR) and FcγRI. By expressing FcγRI and its signaling chain in conventional CD4⁺ T cells, we successfully employed this mechanism to treat established solid cancers. Overall, this discovery sheds new light on the biology of this T cell subset, their function during tumor immunity, and the means to utilize their unique killing signals in immunotherapy.

Introduction

Over recent decades, researchers exerted tremendous efforts to dissect the biological and clinical roles of immune-cell populations that infiltrate tumors (1–3). While it is widely accepted that increased prevalence of cytotoxic T cells and Th1 cells in tumors correlates with improved clinical outcomes (4), the role of tumor-specific B cells and tumor-binding antibodies remains unclear (5, 6). A large number of studies suggest that a Th2 signature and tumor-binding antibodies promote tumor escape through various mechanisms, including masking T cell epitopes (7), inducing suppressor mechanisms (8–11), inducing tumor heterogeneity and therapy resistance (12), altering the tumor microenvironment, increasing tumor proliferation, and promoting angiogenesis (13, 14). In contrast, tumor-binding antibodies were shown to inhibit tumor growth through induction of antibody-dependent cell-mediated cytotoxicity (ADCC) (15), activation of DCs (16, 17), and activation of tumor-infiltrating innate cells (18) and were shown to be required for antitumor T cell activity (19, 20). In the clinic, tumor-binding antibodies are widely used as therapeutic agents (21), and when they arise spontaneously, they correlate with a positive prognosis in several cancers (22, 23). Over the past years, it has become clear that a simple assessment of the titer of tumor-binding antibodies is not sufficient to predict their antitumor effect, as their activity is also dependent on their avidity and affinity (24, 25) and patterns of sialyation, which determine their interactions with Fcγ receptor (FcγR) (26, 27).

By studying spontaneous regression of tumor cells in genetically similar allogeneic hosts (MHC-I and -II matched), we discovered that naturally occurring IgG antibodies enable tumor-associated DCs (TADCs) to activate T cells that recognize a wide range of tumor-associated antigens, including neoantigens (28). Through exploiting this principle, we were able to generate a very potent immunotherapy consisting of a combination of tumor-binding antibodies and DC stimuli (16, 28). Despite eliciting a strong T cell immune response, in this as well as in most immunotherapeutic approaches to cancer, most tumors eventually relapse, probably as a result of intratumor heterogenicity and the capacity of tumors to escape immune pressure by editing the antigens that they express. Therefore, there is a need to develop a therapeutic approach capable of addressing tumor evolution and escape mechanisms.

While searching for ways to enhance the efficacy of antibody-driven cancer immunotherapy, we discovered that CD4⁺ T cells isolated from tumors and tumor-binding antibodies were synergistic in their antitumor effects. This synergy was mediated by a distinct subset of exhausted CD4⁺ T cells that expressed the high-affinity Fcγ receptor (FcγRI) capable of efficiently lysing tumor cells through dual recognition with T cell receptors (TCR) and tumor-binding antibodies. We were able to employ this unique killing mechanism to treat established solid tumors in mouse models, thus diminishing the reliance on the host T cell repertoire.

Results

Adoptive transfer of CD4⁺ T cells, but not CD8⁺ T cells, induces potent tumor regression when combined with tumor-binding antibodies. We recently found that treating tumor-bearing mice with tumor-binding antibodies and DC stimuli induces complete tumor regression through induction of systemic T cell immunity (16, 28). This treatment, however, is limited to tumors smaller than 25 mm^2 and is largely ineffective once tumors exceed that size. In attempts

Conflict of interest: The authors have declared that no conflict of interest exists.

Submitted: January 23, 2019; **Accepted:** July 3, 2019; **Published:** August 26, 2019.
Reference information: *J Clin Invest*. 2019;129(10):4151–4164.
https://doi.org/10.1172/JCI127590.

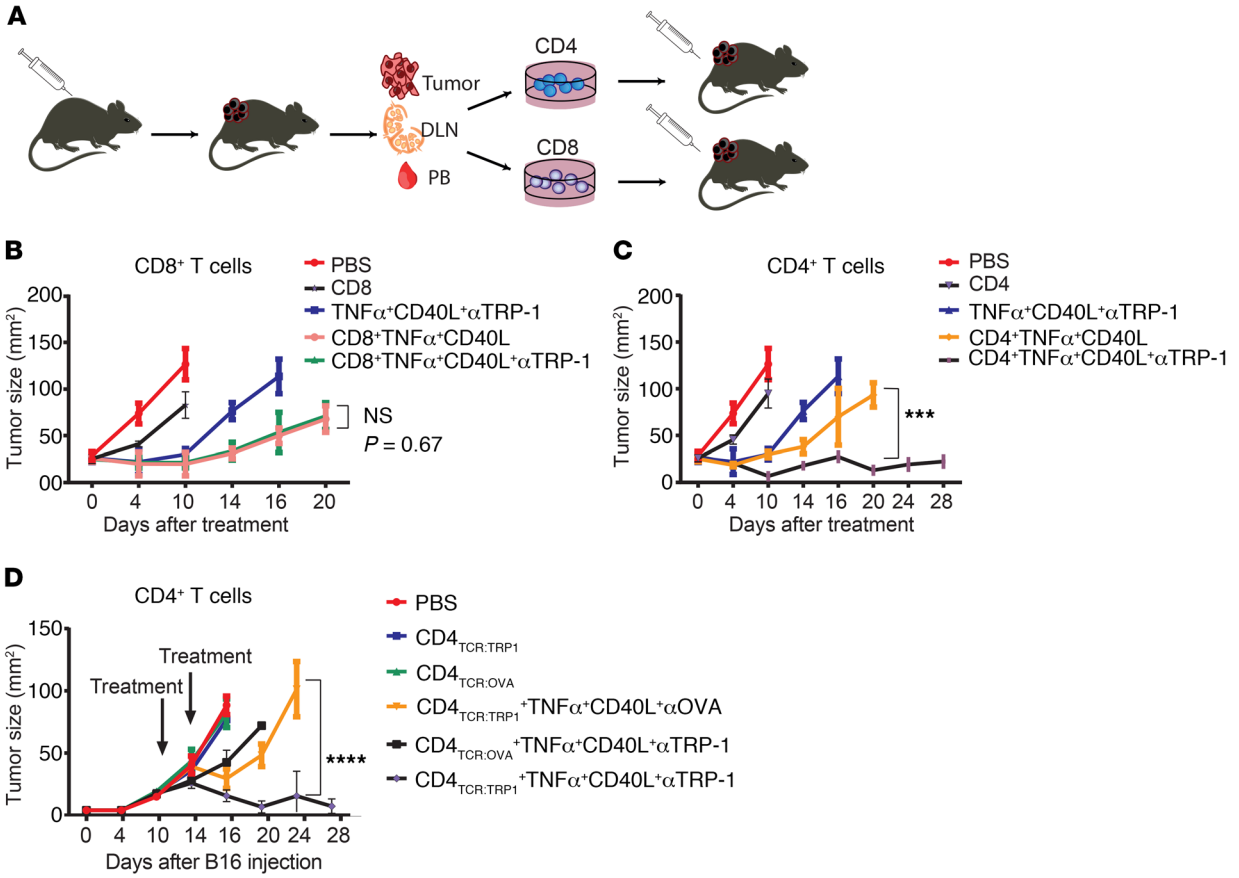

Figure 1. Adoptive transfer of CD4⁺ T cells with tumor-binding antibodies induces direct killing of tumor cells. (**A**) Illustration of experimental outline. (**B**) B16F10 tumor size (mm²) in WT mice following injection of CD8⁺ T cells isolated from day 7 tumor-bearing mice with or without antibodies against TRP-1 and DC stimuli (n = 4). (**C**) B16F10 tumor size (mm²) in WT mice following injection of CD4⁺ T cells isolated from day 7 tumor-bearing mice with or without antibodies against TRP-1 and DC stimuli (n = 4). The same control groups, PBS and TNF-α⁺CD40L⁺αTRP-1, were used in both **B** and **C**. (**D**) B16F10 tumor size (mm²) following adoptive transfer of CD4⁺ T clones, with or without DC stimuli and antibodies against TRP-1 and ovalbumin (n = 4). Results are from 1 representative experiment out of at least 3 performed. Statistical significance was calculated using 2-way ANOVA with post hoc Tukey's test. ***P < 0.001; ****P < 0.0001. P < 0.05 was considered significant.

to improve the potency and durability of tumor-binding antibody therapy, we initially tested it in combination with effector CD8⁺ or CD4⁺ T cells.

For this aim, control mice were injected s.c. with B16 melanoma cells. Ten days following implantation, mice were injected intratumorally with antibodies against the melanoma antigen TRP1 (anti-TRP1), anti-CD40, and TNF-α (DC stimuli). After 6 days, effector (CD62L^{neg}CD44⁺) CD4⁺ and CD8⁺ T cells were isolated from the tumors, blood, and draining lymph nodes (DLN) of treated tumor-bearing mice. T cells were expanded for 7 days in vitro using high-dose IL-2 and anti-CD3 antibodies and injected i.v. into tumor-bearing mice alone or in combination with anti-TRP1 antibodies and with or without DC stimuli (the experimental design is illustrated in Figure 1A). Adoptive transfer of CD8⁺ T cells had only a marginal effect on tumor growth, which was comparable to that in PBS-treated mice. Intratumoral injection of DC stimuli and anti-TRP1 induced marked, yet transient, tumor regression, and most treated mice developed recurrent tumors after 10 to 12 days. Combined injection of DC stimuli with or without anti-TRP1 and with CD8⁺ T cells induced marked tumor regression. However, all mice experienced recurrent tumors after 16 days and needed to be euthanized by day 20 (Figure 1B). Adoptive transfer of CD4⁺ T cells alone yielded no significant improvement over PBS-treated mice. Addition of DC stimuli increased the potency of injected CD4⁺ T cells, but all tumors eventually progressed. Strikingly, however, injection of DC stimuli with anti-TRP1 antibodies substantial improved tumor regression induced by adoptive transfer of CD4⁺ T cells. Furthermore, all mice treated with CD4⁺ T cells along with DC stimuli and anti-TRP1 experienced sustained tumor regression and remained tumor free for the duration of the experiment (Figure 1C).

Next, we tested to determine whether specificity of the antibodies or T cells for tumor antigens is required for CD4⁺ T cell–mediated tumor regression. Toward this end, control mice were injected with B16 and tumors were allowed to grow for 10 days. Mice were then injected i.v. with effector CD4⁺ T cells bearing a single TCR against ovalbumin, which is not expressed on B16, or against the melanoma antigen TRP1. Additionally, mice were injected with DC stimuli and with antibodies against TRP1 or against ovalbumin. Adoptive transfer of effector CD4⁺ T cells alone yielded tumor growth comparable to that seen in

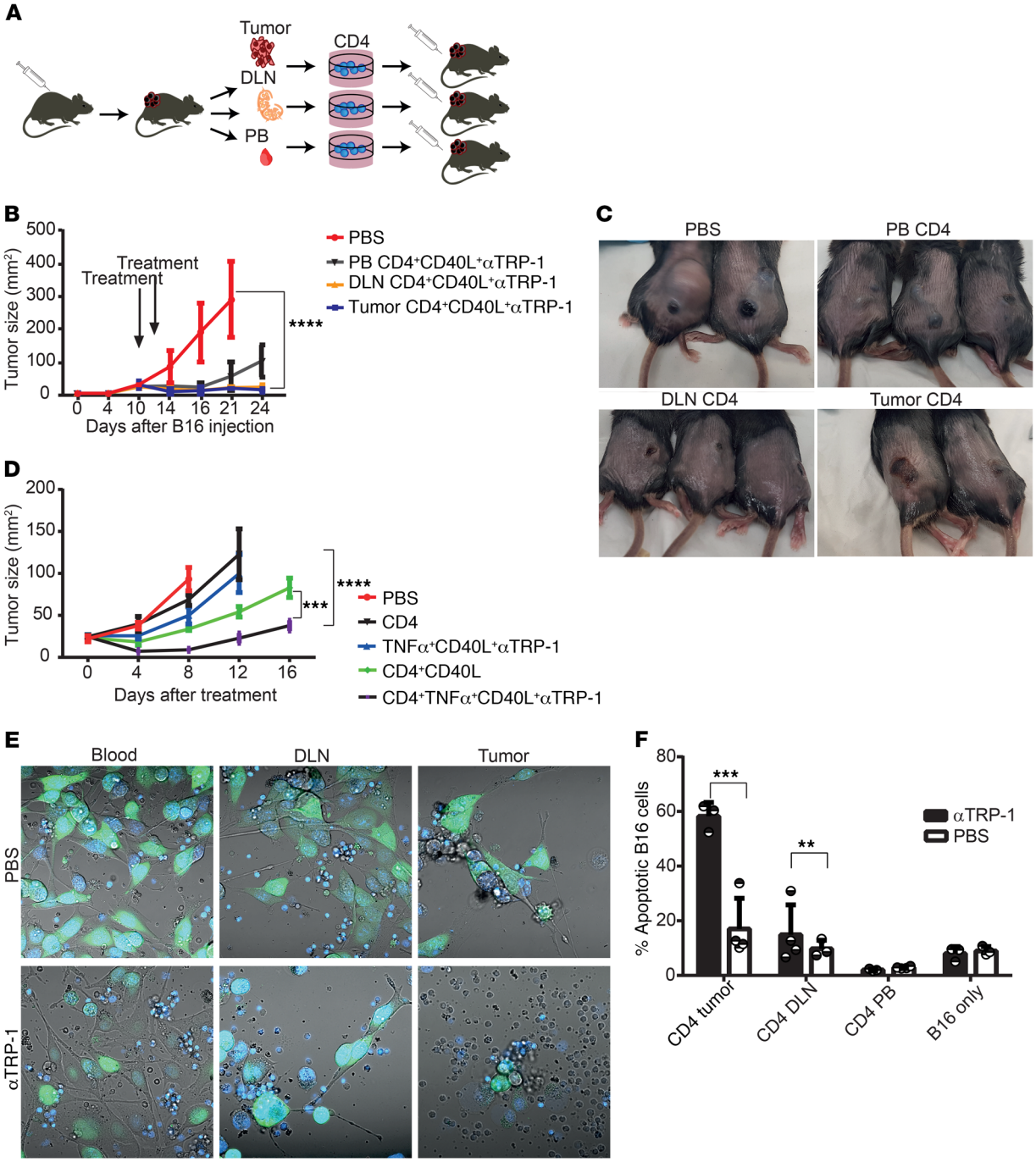

Figure 2. CD4⁺ T cells from the tumor and DLN directly kill tumor cells coated with IgG. (**A**) Illustration of experimental outline. (**B**) B16F10 tumor size (mm^2) in mice following injection of CD4⁺ T cells from day 7 tumor-bearing mice with anti-TRP1 and DC stimuli ($n = 3$). (**C**) Representative photomicrographs of tumor-bearing mice 7 days after adoptive transfer of CD4⁺ T cells. (**D**) B16F10 tumor size (mm^2) in RAG-deficient mice following adoptive transfer of CD4⁺ T cells, with or without antibodies against TRP1 and DC stimuli ($n = 4$). (**E**) Confocal images of wasabi-labeled B16 tumor cells cocultured for 48 hours with CD4⁺ T cells obtained from day 7 tumor-bearing mice. Original magnification, ×800. (**F**) Percentages of dead tumor cells after 48 hours incubation with CD4⁺ T cells measured by flow cytometry analysis of annexin V/PI staining ($n = 3$). Data represent mean ± SEM, and the results are from 1 representative experiment out of at least 3 performed. Statistical significance was calculated using 2-way ANOVA with post hoc Tukey's test $^{**}P < 0.01$; $^{***}P < 0.001$; $^{****}P < 0.0001$. $P < 0.05$ was considered significant.

untreated mice. Similarly, injection of $Ova_{323–339}$–reactive CD4⁺ T cells with anti-ovalbumin or anti-TRP1 antibodies had only a marginal effect on tumor progression. In contrast, injection of TRP1-reactive CD4⁺ T cells along with anti-TRP1, but not anti-ovalbumin, antibodies induced complete and durable tumor regression (Figure 1D). Taken jointly, these results suggest that effector CD4⁺ T cells, but not CD8⁺ T cells, synergize with tumor-reactive antibodies to eradicate tumors in a manner that relies upon the antigen specificity of both the antibodies and T cells.

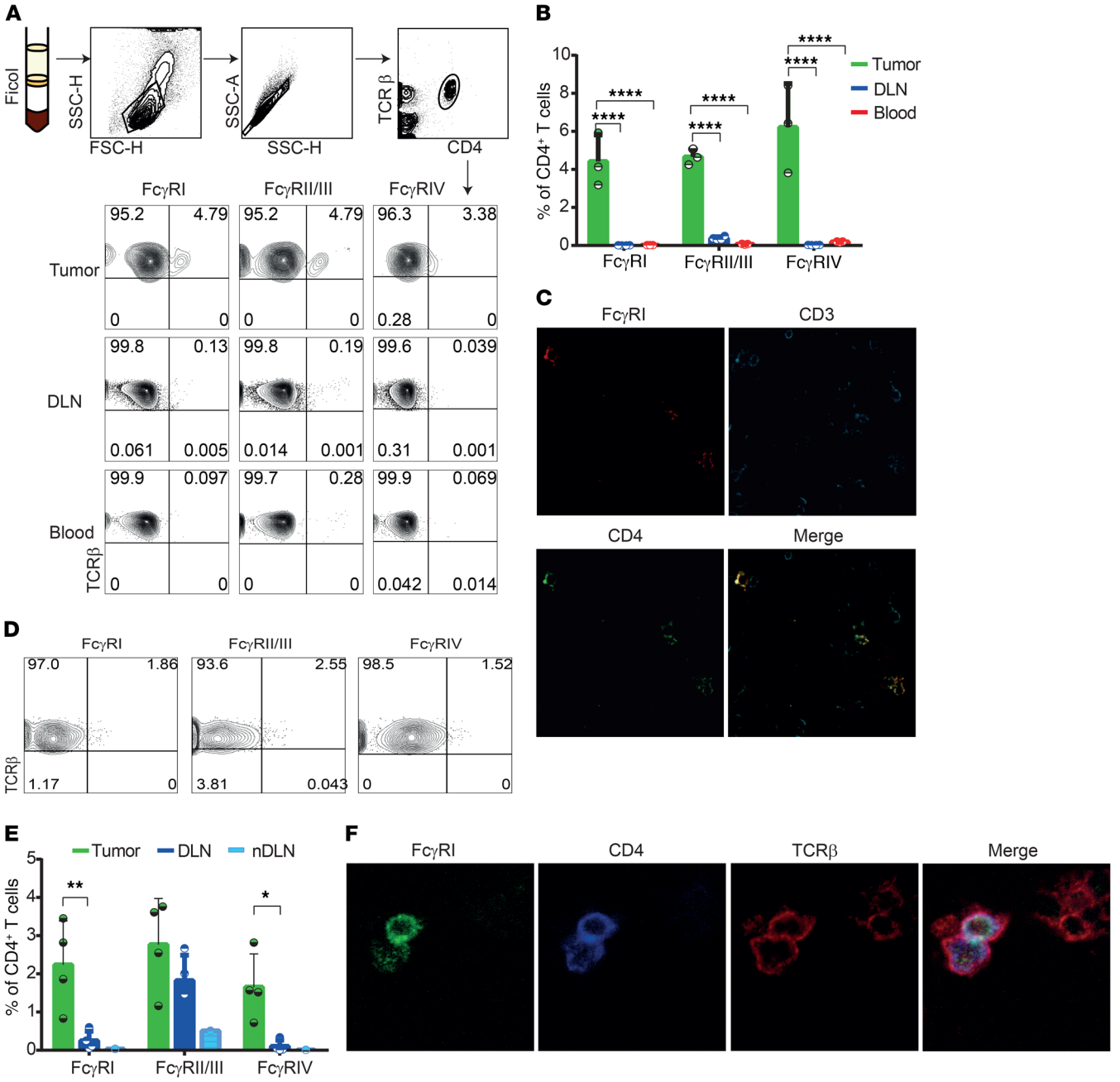

Figure 3. A small subset of tumor-infiltrating CD4⁺ T cells expresses Fcγ receptors. (**A**) Gating strategy and representative FACS analyses of the tumor, DLN, and blood from day-10 tumor-bearing mice. (**B**) Mean percentages of Fcγ receptors expressing CD4⁺ T cells in various organs in day-10 B16 tumor–bearing mice (n = 4). Statistical significance was calculated using 2-way ANOVA with post hoc Tukey's test. (**C**) Confocal microscopy of day-10 B16F10 tumor. Original magnification, ×800. (**D**) Representative FACS analysis of Fcγ receptors on 4T1 tumor-infiltrating CD4⁺ T cells. (**E**) Mean percentages of Fcγ receptors expressing CD4⁺ T cells in various organs in day-12 4T1 tumor-bearing mice (n = 4). Statistical significance was calculated using 2-way ANOVA with post hoc Bonferroni's test. nDLN, nondraining lymph node. (**F**) Confocal microscopy of day-12 4T1 tumor sections. Original magnification, ×800. Data represent mean ± SEM, and results are from 1 representative experiment out of at least 3 performed. *P < 0.05; **P < 0.01; ****P < 0.0001. P < 0.05 was considered significant.

CD4⁺ T cells from the tumor and DLN, but not from peripheral blood, directly kill tumor cells coated with IgG antibodies. Since the above experiments included effector CD4⁺ T cells that were pooled from the blood, tumors, and DLN, we next sought to determine which of these organs contains the most potent tumor-reactive CD4⁺ T cells. We isolated effector CD4⁺ T cells from the blood, DLN, and tumors individually following immunotherapy and expanded them in vitro using IL-2 and anti-CD3. T cells from each organ were injected i.v. into B16 tumor–bearing mice, in combination with DC stimuli and anti-TRP1 antibodies (illustrated in Figure 2A). Effector CD4⁺ T cells from blood had only a moderate effect on tumor burden in these mice compared with in untreated mice, and all treated mice experienced local tumor recurrence and had to be sacrificed. In contrast, injection of CD4⁺ T cells isolated

from the tumor or DLN induced complete tumor regression that was maintained until the experiment was terminated (Figure 2, B and C). We next assessed whether transferred $CD4^+$ T cells kill tumor cells directly or mediate killing by activating other effector T cells. Thus, Rag1-deficient mice ($Rag1^{-/-}$) were challenged with B16 cells, and tumors were allowed to grow for 10 days. Mice were then treated with 1×10^6 $CD4^+$ T cells derived from tumor-bearing mice treated with immunotherapy along with tumor-binding antibodies and DC stimuli. Interestingly, the efficacy of this treatment in $Rag1^{-/-}$ mice was comparable to that in immune-competent mice, suggesting that tumor lysis is induced directly by the injected $CD4^+$ cells (Figure 2D). Additionally, we isolated $CD4^+$ T cells from the blood, DLN, and tumor of B16 tumor–bearing mice and cocultured them with B16 cells in the presence or absence of anti-TRP1 antibodies. Incubation of $CD4^+$ T cells from all organs with tumor cells at a 1 to 2 ratio, in the absence of antibodies, exhibited minimal effect; about 10% of tumor cell lysis was observed. Consistent with our in vivo observations, incubation of tumor cells coated with antibodies and $CD4^+$ T cells from tumors, and to a lesser extent also from the DLN, but not from the blood, induced tumor cell lysis within 2 days (Figure 2, E and F, and Supplemental Figure 1A; supplemental material available online with this article; https://doi.org/10.1172/JCI127590DS1). Since $CD4^+$ T cells express the C5a and C3b complement receptors, we next tested to determine whether the tumor lysis is mediated by complement deposition. To eliminate any potential inactivated complement, $CD4^+$ T cells were incubated with IgG-coated tumor cells in the absence of serum. Only a minor reduction in tumor cell lysis was observed, suggesting a direct IgG binding by $CD4^+$ T cells (Supplemental Figure 1B).

A small subset of $CD4^+$ T cells in tumors and DLNs express Fcγ receptors. Although it is widely believed that T cells do not express Fcγ receptors (FcγR), in light of our results, we decided to revisit this notion. Toward this end, tumors, DLN, and peripheral blood (PB) were obtained from B16 tumor–bearing mice 10 days following tumor inoculation, and expression patterns of FcγR (FcγRI, FcγRII/III, and FcγRIV) on $CD4^+$ T cells were analyzed. Flow cytometric analysis indicated that between 3% and 5% of the tumor-infiltrating $CD4^+$ T cells expressed all FcγR at levels comparable to those of antigen-presenting myeloid cells (Figure 3, A and B, and Supplemental Figure 2, A and B). Lower yet detectable percentages of $CD4^+$ T cells expressing FcγR were also observed in the DLN, but not in the blood (Figure 3, A and B). To further corroborate these results, histological sections of day-10 B16 tumors were stained for FcγR and T cell markers. Indeed, all FcγRs were detected on a proportion of $CD4^+$ but not $CD8^+$ T cells (Figure 3C and Supplemental Figure 2C).

We then tested to determine whether this $FcγR^+$ subset exists in another tumor model or is limited to B16 melanoma. Female BALB/c mice were injected with 4T1 breast cancer cells into their mammary fat pad, and tumors were allowed to grow for 12 days. Similarly to our results with B16 cells in C57BL/6 mice, all FcγR were expressed on $CD4^+$ T cells in the tumors and DLN of BALB/c mice bearing 4T1 breast carcinoma cells, but not on the T cells in their non-DLNs (Figure 3, D and E). Histological sections of day-12 4T1 tumors confirmed that these receptors are indeed expressed on the membrane of $CD4^+$ T cells (Figure 3F and Supplemental Figure 2D).

Naturally occurring $CD4^+$ T cells expressing FcγRI lyse tumor cells coated with IgG. We next tested to determine whether this population exists in naive mice or is induced exclusively during tumor progression. Various organs were removed from naive mice, and FcγR expression on T cells was analyzed by flow cytometry. Only $CD4^+$ T cells expressing FcγRI and II/III were found in lymph nodes, spleen, and BM, but not in the blood or thymus (Figure 4A and Supplemental Figure 3A). The high-affinity FcγRI was found to be the predominant receptor on T cells, and this population was mostly prevalent in the spleen. Furthermore, histological sections of naive spleen indicated that they are located at the margins of the T cell zone in the spleen of naive mice (Figure 4B). Intracellular staining of the Th transcription factor indicated that T cells expressing FcγRI exclusively express the Th1 T-bet in both spleen and tumors (Figure 4C). This population was completely absent in $Rag1^{-/-}$ mice, suggesting that their maturation is dependent on TCR rearrangement (not shown). Expression of FcγRI in these cells was also tested at the transcription level. To this end, splenocytes were subjected to a Ficoll gradient enriched on CD4 magnetic beads, and $CD4^+CD3^+$TCR-$β^+$MHC-$II^{neg/dim}$ T cells were sorted into 2 groups based on their and FcγRI expression (Figure 4D). mRNA was extracted from the 2 subsets, and FcγRI transcripts were amplified by PCR. Consistent with our FACS and confocal results, $FcγRI^+CD3^+$MHC-$II^{neg/dim}$ $CD4^+$ T cells, but not canonical $CD4^+$ T cells, had low yet detectable levels of FcγRI gene transcript (Figure 4E). To further verify that these are indeed T cells, $CD4^+CD3^+$TCR-$β^+$MHC-$II^{neg/dim}$–expressing $FcγRI^+$ were sorted and compared with canonical $FcγRI^{neg}$ cells by confocal microscopy. The 2 subsets share a similar morphology and size and have identical cell membrane CD4, CD3, and TCR-β staining (Figure 4F and Supplemental Figure 3B). Consistent with our FACS data, confocal staining further indicated that FcγRI is expressed on the membrane of these cells (Figure 4F). Next, we tested to determine whether the expression of FcγR on these cells was functional or merely a surface marker. Splenic $CD4^+$ T cells that either expressed or did not express FcγRI were isolated from control mice and incubated overnight with B16 tumor cells. Incubation of $FcγRI^+CD4^+$, but not canonical $FcγRI^{neg}CD4^+$ T cells, with B16 precoated with anti-TRP1 antibodies induced marked tumor cell lysis (Figure 4, G and H). Tumor cell lysis was completely abrogated when $FcγRI^+CD4^+$ T cells were incubated with anti-ovalbumin antibodies, or anti-TRP1 $F(ab')_2$ (Figure 4, G and H, and Supplemental Figure 3D). Tumor lysis was mediated through secretion of lytic granules in an IFN-γ–dependent mechanism (Supplemental Figure 3D). Intriguingly, incubation of $FcγRI^+CD4^+$ isolated from OT-II mice with B16 and anti-TRP1 did not induce tumor killing, suggesting that the both MHC-II molecules and the antigen targeted by the antibody should be expressed on the target cells (Figure 4, G and H, and Supplemental Figure 3, E and F). Taken jointly, these data suggest that this specific subset of $FcγRI^+CD4^+$ T cells exhibits a unique capacity to lyse tumor cells directly in a manner that is dependent on concomitant TCR and FcγRI crosslinking.

FcγRI is expressed only on a subset of exhausted and nonproliferating $CD4^+$ T cells. To assess the origin of these cells, we tested to determine whether FcγRI $CD4^+$ T cells bear unique TCR, or rather share clones with conventional $CD4^+$ T cells, which do not express FcγRI. 2×10^5 T cells were sorted by FACS, and their TCR-Vα

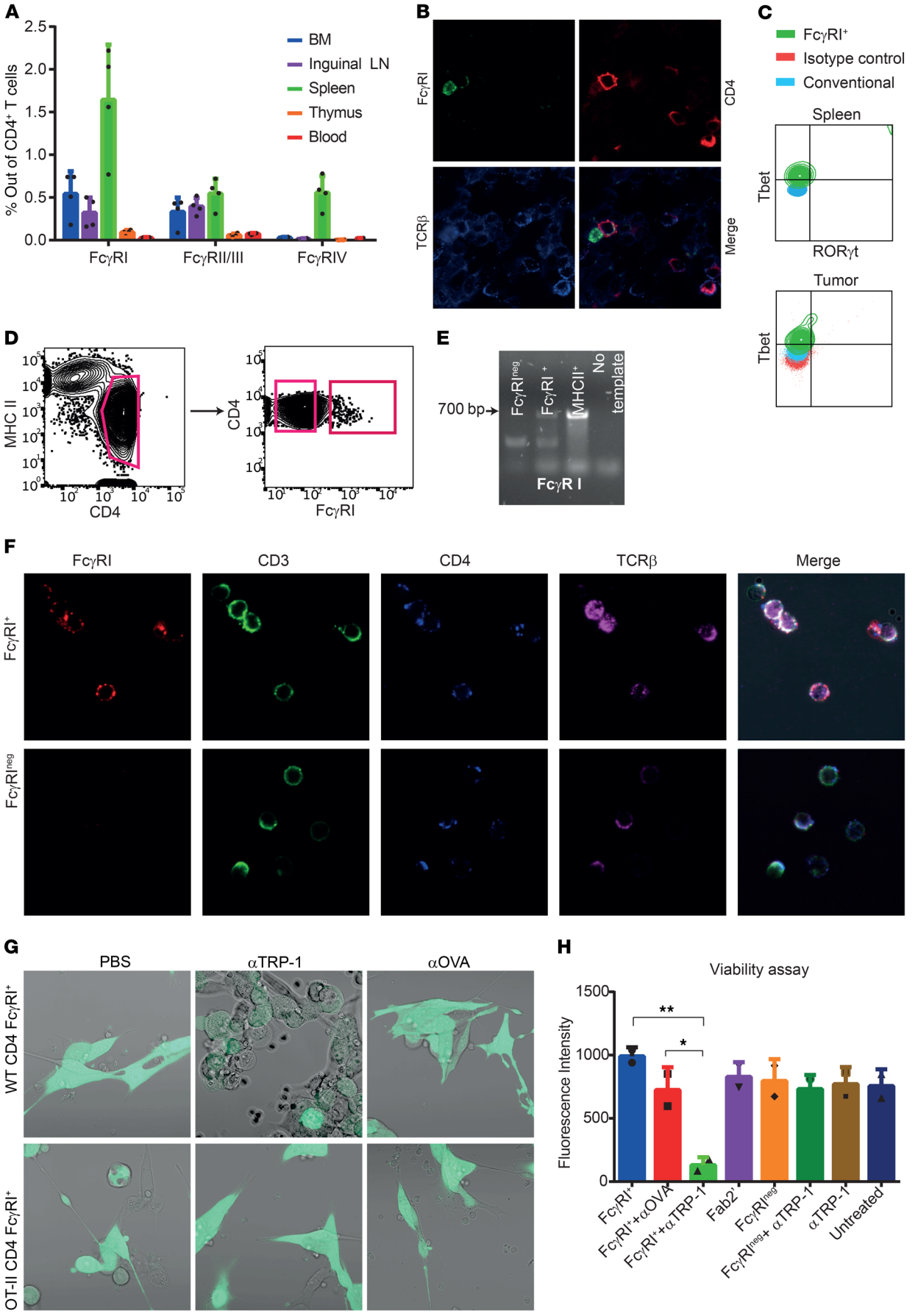
A
% Out of CD4+ T cells
BM
Inguinal LN
Spleen
Thymus
Blood
FcγRI
FcγRII/III
FcγRIV
B
FcγRI
CD4
TCRβ
Merge
C
FcγRI+
Isotype control
Conventional
Spleen
Tbet
RORγt
Tumor
D
MHC II
CD4
FcγRI
E
700 bp
FcγRIneg
FcγRI+
MHCII+
No template
FcγR I
F
FcγRI
CD3
CD4
TCRβ
Merge
FcγRI+
FcγRIneg
G
PBS
αTRP-1
αOVA
WT CD4 FcγRI+
OT-II CD4 FcγRI+
H
Viability assay
Fluorescence Intensity
FcγRI+
FcγRI+αOVA
FcγRI+αTRP-1
Fab2'
FcγRIneg
FcγRIneg+ αTRP-1
αTRP-1
Untreated

Figure 4. Naturally occurring FcγRI⁺-expressing CD4⁺ T cells lyse tumor cells coated with IgG. (**A**) Mean percentages of FcγR-expressing CD4⁺ T cells in different organs from naive mice. (**B**) Confocal microscopy of spleen sections from naive mice. (**C**) Intracellular staining of T-bet and RORγT in naive spleen and tumor-infiltrating CD4⁺ T cells. (**D**) FACS-sorting strategy for FcγRI^{neg} and FcγRI^{pos} CD4⁺ T cells from naive spleens. (**E**) Agarose gel (1%) electrophoresis of FcγRI PCR products performed on cDNA from sorted splenic CD4⁺ T cells. (**F**) Confocal microscopy staining of sorted FcγRI^{neg} and FcγRI^{pos} CD4⁺ T cells. (**G**) Confocal microscopy of CD4⁺ T cells from WT and OT-II mice incubated for 48 hours with wasabi-labeled B16 cells, with or without antibodies against TRP1 and ovalbumin. Original magnification, ×400. (**H**) Viability (measured by fluorescent intensity of wasabi) of B16F10 cells after 48 hours coculture with CD4⁺ T cells (n = 6). Data represent mean ± SEM, and results are from 1 representative experiment out of at least 3 performed. Statistical significance was determined by 1-way ANOVA with Tukey's post hoc test. *P < 0.05; **P < 0.01. P < 0.05 was considered significant.

and -Vβ were amplified by PCR and sequenced. We found that CD4⁺ T cells expressing FcγRI exhibit Vβ segment usage similar to that of conventional CD4⁺ T cells and are composed of hundreds of different clones with frequency distribution and usage, as well as clonal abundance, similar to those of conventional CD4⁺ T cells (Figure 5, A and B). Furthermore, our analysis indicated that identical clones can be found in both groups (Supplemental Table 1). Since both subsets undergo similar random VDJ rearrangement, expression of FcγRI on T cells represents an activation state, rather than expansion of selected clones or T cell subsets with restricted Vβ usage, such as NKT cells. Protein production in these cells was also analyzed by mass spectrometry in comparison with canonical splenic CD4⁺ T cells. The vast majority of detected proteins, including the T markers CD3, CD4, and CD5 as well as the transcription factor NFAT, were expressed at similar levels in both cell populations (Figure 5C and Supplemental Table 2). Several proteins, however, including SYK tyrosine kinase and the chemokine CXCL-4, were detected only in FcγRI⁺CD4⁺ T cells. Of particular interest were the high expression levels of lysosome-related enzymes, suggesting that these cells are more active compared with naive CD4⁺ T cells (Figure 5C).

To assess the hypothesis that FcγR1 expression occurs as a result of activation, canonical CD4⁺ T cells, which do not express FcγRI, were isolated from spleens of naive mice and activated overnight with an array of inflammatory mediators, which induce FcγRI transcription in myeloid cells (29). None of these stimuli induced FcγRI expression on these T cells (Figure 5D). Since incubating FcγRI⁺CD4⁺ T cells with high-dose IL-2 and immobilized anti-CD3 antibodies did not result in their proliferation in vitro (not shown), we speculated that FcγRI may be expressed on exhausted cells. Thus, CD4⁺ T cells from the spleen and lymph nodes of naive mice were cultured for 12 days with immobilized anti-CD3 antibodies and IL-2, followed by an additional 48 hours of activation with PMA and ionomycin. Given the high mortality rate of mouse T cells following such long-term culture and activation, special attention was given to exclude dying T cells (our gating strategy is presented in Figure 5E). Indeed, over 40% of long-term activated CD4⁺ T cells expressed FcγRI, suggesting that its expression is associated with reduced proliferative capacity (Figure 5F). While the majority of long-term activated CD4⁺ T cells expressed exhausted markers, only about 50% of them also expressed FcγRI. Additionally, the majority of, but not all, CD4⁺ T cells that expressed FcγRI also express exhausted markers (Figure 5G). While these results strongly support the hypothesis that CD4⁺ T cells may express FcγRI once they become exhausted and lose their proliferative capacity, the exact underlying mechanism is not fully clear yet.

Canonical T cells equipped with FcγRI exert cytotoxic activities and can be employed to eradicate solid tumors. Since FcγRI⁺CD4⁺ T cells could not be expanded to numbers that allow their use for immunotherapy, we tested to determine whether their killing machinery could be transferred to conventional CD4⁺ T cells. Thus, we transduced conventional splenic CD4⁺ T cells with TRP1-reactive TCR alone or with FcγRI α chain (FcRα) and with the FcεRIγ, which is the receptor signaling γ chain (FcRγ). Transduced T cells were sorted by FACS (Supplemental Figure 4A) and incubated overnight with B16 tumor cells. Membrane-bound CD107a was detected in about 10% of CD4⁺ T cells infected with TRP1-reactive TCR, and they induced about 10% to 15% killing (Figure 6, A and B). Their killing capacities and membrane CD107a levels were not changed by the addition of anti-TRP1 antibodies. Infection with α chain alone was not sufficient to promote B16 lysis and CD107a expression, yet addition of FcRγ substantially potentiated their capacity to lyse antibody-coated tumor cells. Most strikingly, CD4⁺ T cells transduced with TRP1-reactive TCR, FcγRI, and FcRγ induced substantial killing of tumor cells coated with anti-TRP1 antibodies (Figure 6, A and B, and Supplemental Figure 4, B and C). To determine whether the killing capacities of TRP-1–reactive T cells are restricted to anti-TRP1 antibodies, we also coated B16 cells with antibodies against another melanoma antigen, TRP-2. Similarly to our results with anti-TRP1 antibodies, the addition of anti-TRP2 antibodies significantly enhanced the cytotoxic abilities of TRP-1–reactive T cells, suggesting that this killing mechanism is not restricted to a certain antibody (Figure 6C). We then assessed the capacity of these cells to eradicate established melanoma tumors. Mice were injected s.c. with B16 tumor cells, and tumors were allowed to grow for 7 to 9 days, until they reached a palpable size. 0.5×10^6 CD4⁺ T cells were injected i.v., with or without i.p. injection of antibodies. Mice injected with 1×10^6 of CD4⁺ T cells bearing TRP1-reactive TCR served as controls. Consistent with their activity in vitro, combination of TRP1-reactive TCR, FcγRI, and FcRγ T cells and anti-TRP1 antibodies induced tumor eradication in all treated mice that lasted up to 1 month, when the experiment was terminated (Figure 6, D and E). However, many cell types in the tumor microenvironment, such as macrophages and NK cells, express FcγR and can kill tumor cells coated with antibodies. Therefore, we sought to determine whether the synergism between CD4⁺ T cells and tumor-binding antibodies is mediated through the crosslinking of FcγRI on the T cells or rather in an unrelated manner by activating other effector cells at the tumor site. Toward this end, C57 control mice were injected for 3 days with 30 mg/kg of busulfan and rescued with 15×10^6 BM cells from FcεRIγ KO mice, which lack all FcγR. After 3 weeks, the mice were challenged with B16F10 tumor cells, and tumors were allowed to grow for 7 to 9 days until they reached a palpable size. Chimeric mice were then injected with 1×10^6 CD4⁺ T cells bearing TRP1-reactive TCR FcγRI and FcRγ served and with or without anti-TRP1 antibodies. Consistent with our results in

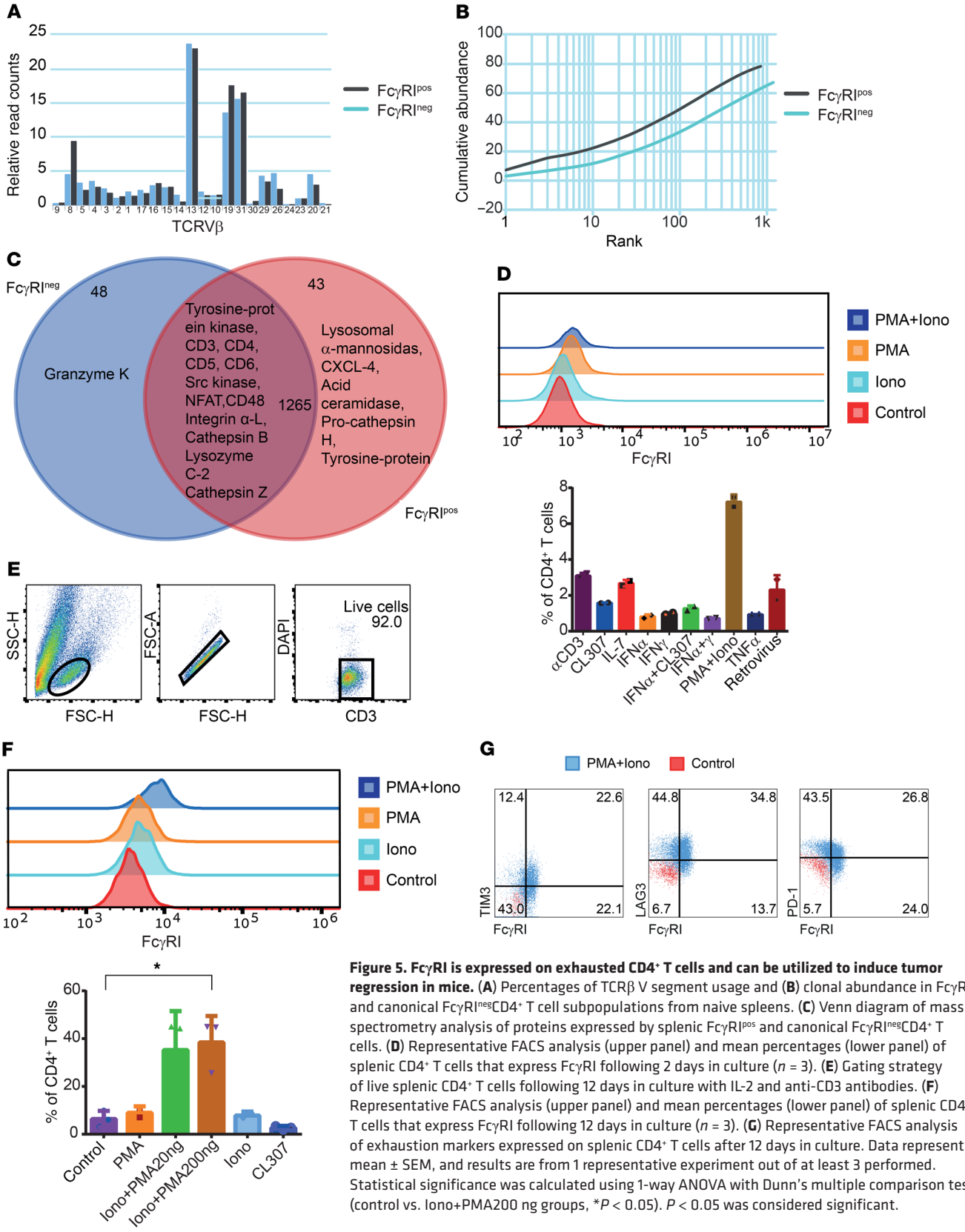

Figure 5. FcγRI is expressed on exhausted CD4⁺ T cells and can be utilized to induce tumor regression in mice. (**A**) Percentages of TCRβ V segment usage and (**B**) clonal abundance in FcγRI⁺ and canonical FcγRI^{neg}CD4⁺ T cell subpopulations from naive spleens. (**C**) Venn diagram of mass spectrometry analysis of proteins expressed by splenic FcγRI^{pos} and canonical FcγRI^{neg}CD4⁺ T cells. (**D**) Representative FACS analysis (upper panel) and mean percentages (lower panel) of splenic CD4⁺ T cells that express FcγRI following 2 days in culture (n = 3). (**E**) Gating strategy of live splenic CD4⁺ T cells following 12 days in culture with IL-2 and anti-CD3 antibodies. (**F**) Representative FACS analysis (upper panel) and mean percentages (lower panel) of splenic CD4⁺ T cells that express FcγRI following 12 days in culture (n = 3). (**G**) Representative FACS analysis of exhaustion markers expressed on splenic CD4⁺ T cells after 12 days in culture. Data represent mean ± SEM, and results are from 1 representative experiment out of at least 3 performed. Statistical significance was calculated using 1-way ANOVA with Dunn's multiple comparison test (control vs. Iono+PMA200 ng groups, *P < 0.05). P < 0.05 was considered significant.

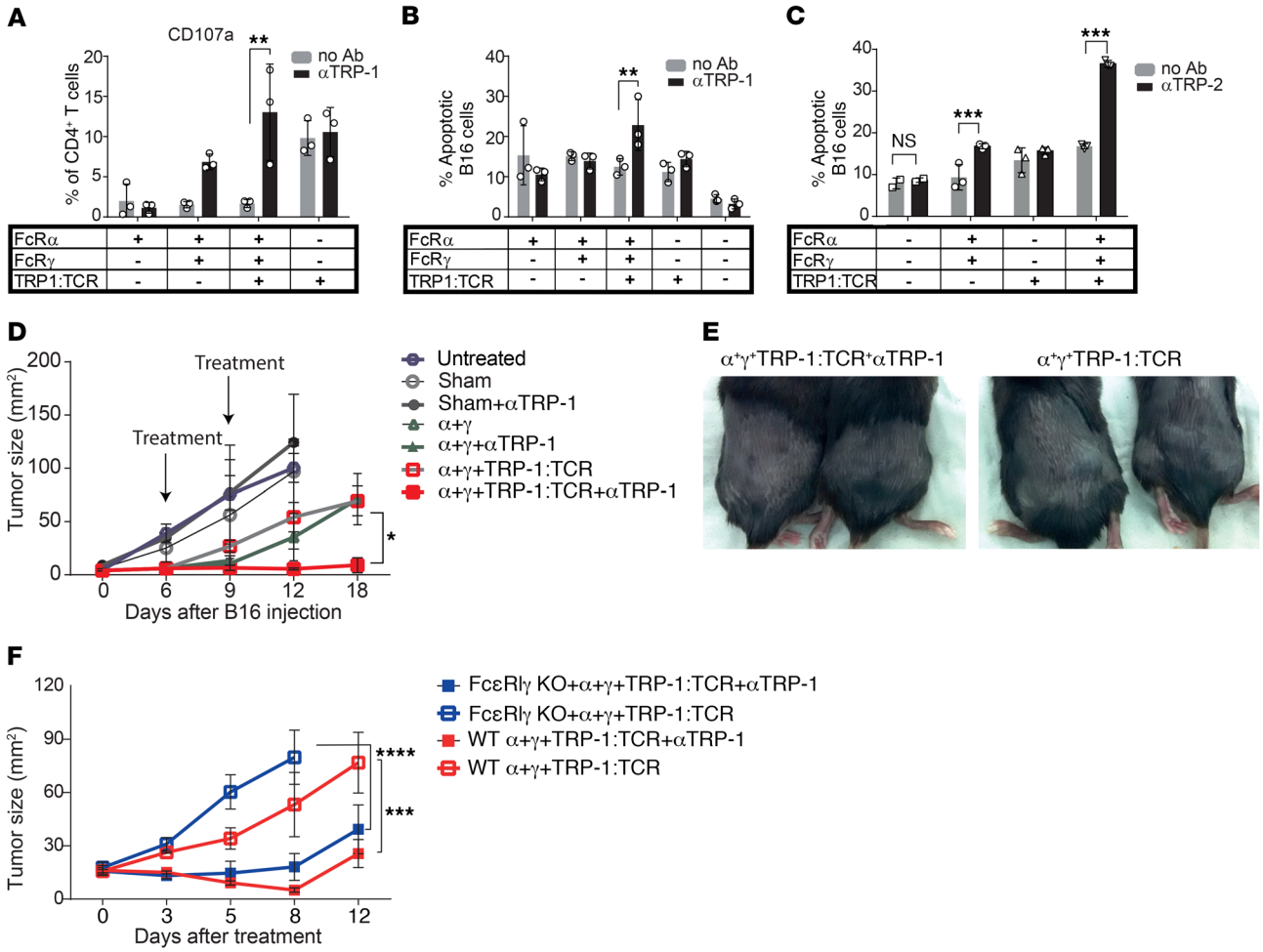

Figure 6. Ectopic expression of FcγRI in canonical T cells endows cytotoxic activity and can be employed to eradicate solid tumors. (**A**) Mean percentages of membrane-bound CD107a in infected splenic CD4$^+$ T cells cultured for 48 hours with B16 tumor cells. (**B**) Mean percentages of apoptotic B16 cells as indicated by annexin V/PI staining following 48 hours incubation with infected CD4$^+$ T cells (n = 3). (**C**) Mean percentages of apoptotic B16 cells as indicated by annexin V/PI staining following 48 hours incubation with CD4$^+$ T cells cultured for 48 hours with B16 tumor cells. (**D**) B16F10 tumor size (mm^2) following adoptive transfer of transduced CD4$^+$ T cells (n = 4). (**E**) Photomicrographs of tumor-bearing mice 12 days after adoptive transfer of infected CD4$^+$ T cells. (**F**) B16F10 tumor size (mm^2) in chimeric mice bearing BM from control (red lines) or from FcεRIγ KO mice (blue lines) following adoptive transfer of transduced CD4$^+$ T cells (n = 4). Data represent mean ± SD, and results are from 1 representative experiment out of at least 3 performed. Statistical significance was calculated using 2-way ANOVA with post hoc Šidák's multiple comparisons test for **A**, **B**, and **C**, and Tukey's comparisons test for **D** and **F**. *P < 0.05; **P < 0.01; ***P < 0.001; ****P < 0.0001. P < 0.05 was considered significant.

control mice, a significant tumor regression was observed following treatment with both T cells and antibodies, suggesting direct activation of T cells by tumor-binding antibodies (Figure 6F).

FcγRI$^+$ is expressed by CD4$^+$ T cells that infiltrate to human tumors. We also tested to determine whether CD4$^+$ T cells expressing FcγRI are limited to mice or can also be found in humans. Initially, FcγR expression was tested on T cells from PB of 4 healthy donors. Consistent with our results in mice, we could not detect T cells expressing Fcγ receptors even after their activation for 3 days with PMA and ionomycin (Figure 7A). In contrast to our results in mice, long-term activation with IL-2 and anti-CD3 antibodies followed by 2 days activation with PMA and ionomycin did not induce FcγR expression of blood T cells (Figure 7B). Next, tumor tissues from stage III melanoma patients undergoing primary tumor resection were analyzed by FACS and by histological staining. FACS analysis indicated the presence of tumor-infiltrating CD4$^+$, but not CD8$^+$, T cells, expressing all 3 FcγRs (Figure 7C). Examination of tumor sections under confocal microscopy further indicated that these receptors are expressed on the membrane of CD4$^+$ T cells and that these cells are found in the center of the tumor mass (Figure 7D and Supplemental Figure 5A). In another patient undergoing resection surgery to remove stage III bladder cancer following chemotherapy, we compared the expression patterns of FcγR on CD4$^+$ T cells in the blood, tumor tissue, and adjacent healthy bladder tissue. Low yet detectable levels of FcγRI and FcγRIII, but not FcγRII, were found in circulating CD4$^+$ T cells (Figure 7E). Importantly, all 3 FcγRs were detected on CD4$^+$ T cells infiltrating the tumor, but not in healthy tissue (Figure 7F and Supplemental Figure 5B). CD4$^+$ T cells expressing all FcγRs were found in the tumor of another melanoma patient, thus demonstrating that these cells preferentially accumulate in cancerous tissues (Figure 7G).

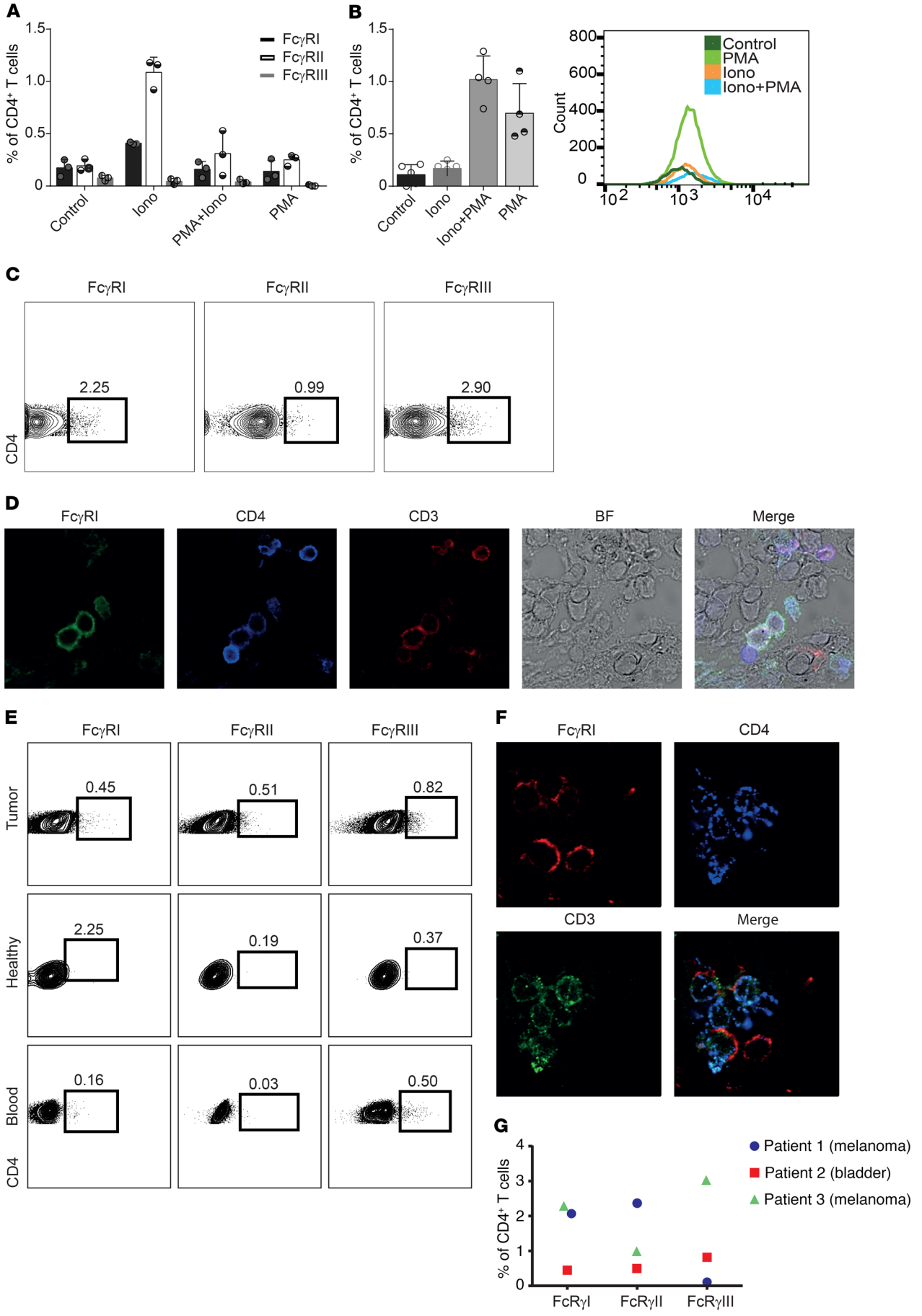
A
% of CD4+ T cells
FcγRI
FcγRII
FcγRIII
Control
Iono
PMA+Iono
PMA
B
% of CD4+ T cells
Control
Iono
Iono+PMA
PMA
Count
Control
PMA
Iono
Iono+PMA
C
FcγRI
FcγRII
FcγRIII
2.25
0.99
2.90
CD4
D
FcγRI
CD4
CD3
BF
Merge
E
FcγRI
FcγRII
FcγRIII
Tumor
0.45
0.51
0.82
Healthy
2.25
0.19
0.37
Blood
0.16
0.03
0.50
CD4
F
FcγRI
CD4
CD3
Merge
G
% of CD4+ T cells
FcRγI
FcRγII
FcRγIII
Patient 1 (melanoma)
Patient 2 (bladder)
Patient 3 (melanoma)

Figure 7. FcγR expressing CD4⁺ T cells are also found in human tumors. (**A**) Mean percentages of FcγR expression in CD4⁺ T cells from PB of healthy donors. (**B**) Mean percentages of FcγRI expression in CD4⁺ T cells from PB of healthy donors after 28-day culture with IL-2 and anti-CD3 antibodies. (**C**) FACS analysis of FcγR expression on CD4⁺ T cells from tumor lesion of a stage IIb melanoma patient. (**D**) Confocal microscopy of a histological section from the same stage IIb melanoma patient as in **C**. Original magnification, ×600. (**E**) FcγR expression in CD4⁺ T cells from the blood, tumor, and healthy adjacent tissue of a stage III bladder cancer patient. (**F**) Confocal microscopy staining of FcγRI in a histological section of the same bladder cancer patient as in **E**. Original magnification, ×800. (**G**) Percentages of FcγR-expressing CD4⁺ T cells in tumors from 3 patients.

Discussion

Whether tumor-binding IgG promotes or masks T cell immunity is still controversial (5, 6), and several studies have demonstrated that they can inhibit cytotoxic T cell activity by promoting mechanisms of immune suppression (7–11, 13, 14, 30). In contrast, however, tumor-binding antibodies are extensively used in the clinic (21), and a large amount of experimental data compellingly suggest that they synergize and promote T cell immunity (15, 19, 20). Here, we found that tumor-reactive CD4⁺ T cells and tumor-binding antibodies strongly synergize to mediate tumor regression. This synergy is mediated by a distinct CD4⁺ T cell population, which expresses the high-affinity FcγRI and directly kills tumor cells coated with antibodies.

Whether or not T cells express Fcγ receptors has been a source of long-lasting controversy (31). While conventional wisdom suggests that T cells do not express them (32), a number of studies have found that activated T cells in the PB of patients with systemic lupus erythematosus (SLE) or with cytomegalovirus infections express the low-affinity FcγRIII. Since the authors could not detect them in the blood of healthy donors, they concluded that the cells were in an activated state caused by exposure to IFN-γ (33). We found that a short-term activation with double-stranded RNA, or with type I or II IFN, was not sufficient to induce FcγRI expression on CD4⁺ T cells. CD4⁺, but not CD8⁺, T cells appear to elevate their FcγRI expression only once they have completely lost their proliferative capacities.

Our findings also suggest a direct cytotoxic activity of tumor-infiltrating CD4⁺ T cells. While effector Th1 CD4⁺ T cells are highly associated with increased antitumor immunity and improved clinical outcomes (23, 34), most of the publications attributed the antitumor effects of CD4⁺ T cells to their capacity to activate other effector cells, in particular, cytotoxic CD8⁺ T cells (35, 36). Indeed, CD4⁺ T cells were shown to promote differentiation and clonal expansion of tumor-reactive T cells and are essential for maintaining and reactivating CD8⁺ memory T cells (37–39). In the clinical setting, Hunder et al. reported a case in which infusion of autologous CD4⁺ T cell clones against class II–restricted epitopes led to a long-term complete remission of refractory melanoma (40). In a more recent case report, Tran et al. demonstrated transient regression of all metastases following injection of tumor-infiltrating CD4⁺ T cells that recognize mutated ERBB2IP (41). A number of independent studies have shown that CD4⁺ T cells can mediate the direct killing of melanoma cells. Muranski et al. were the first to demonstrate such a phenomenon through their capacity to secrete perforin and granzyme (42). Alternately, cytotoxic CD4⁺ T cells that express NKG2A have also been reported in mice (43, 44) and in human melanoma (45). Nonetheless, the relevance of their findings to other tumors remains somewhat questionable, mainly since MHC-II expression on melanoma is diverse and not uniform. Consistently, we found that incubation of tumor cell lines that do not express MHC-II molecules, such as 4T1, with CD4⁺ T cells expressing FcγRI, is not sufficient to induce tumor cell killing in the presence of tumor-binding antibodies. These results, therefore, strongly support the notion that the killing machinery of such cells is still dependent on TCR specificity. In that regard, the role of FcγRI-antibody interactions in facilitating killing through TCR could involve stabilizing the low-affinity complexes of TCR and MHC peptides. Presumably, a direct correlation exists between the avidity of the tumor-binding antibodies and T cell killing efficacy.

Overall, this work highlights a surprising synergy between tumor-binding antibodies and CD4⁺ T cells in lysing tumor cells and positions them as a therapeutic agent — a role that surpasses their traditional one as supporting the cytotoxic activities of other effector cells.

Methods

Mice. WT C57BL/6J and BALB/cOlaHsd mice were obtained from Envigo and from Jackson Laboratory. T cell–deficient mice B6.Cg-Rag1^{tm1Mom} and TCR transgenic mice Tyrp1B-w Tg(Tcrα, Tcrβ)9Rest/J were purchased from Jackson Laboratory. B6.Cg-Tg (Tcrα,Tcrβ)425Cbn/J were purchased from Jackson Laboratory or provided by Ronen Alon (Weizmann Institute, Rehovot, Israel). B6;129P2-FcεRIγ^{tm1Rav}/J mice were provided by Rony Dahan (Weizmann Institute). Male and female 8- to 12-week-old mice were used in all experiments.

Cell lines. B16F10 cells (CRL-6475) and 4T1 (CRL-2539) cells were purchased from ATCC, and HEK-293FT cells were purchased from Thermo Fisher Scientific, all in January 2017. Cells were cultured in DMEM (Gibco, Thermo Fisher Scientific) supplemented with 10% heat-inactivated FBS (Biological Industries), 2 mM L-glutamine, and 100 μg/mL penicillin/streptomycin (Gibco, Thermo Fisher Scientific) under standard conditions. Cells were routinely tested for mycoplasma using a EZ-PCR Mycoplasma Test Kit (Biological Industries) according to the manufacturer's instructions.

In vivo tumor models. For melanoma tumor studies, 2×10^5 B16F10 cells suspended in 50 μL were injected s.c. into C57BL/6 mice above the right flank, and the size of growing tumors was measured twice a week using calipers. Treatment was applied at days 8 and 12 after injection or when tumors reached 20 mm^2 (day 0 and day 4). When tumors reached 120 mm^2, the mice were sacrificed due to ethical considerations. For a triple-negative breast cancer model, 2×10^5 4T1 cells in 30 μL DMEM were injected into fat pad number 5 of a 12-week-old female BALB/c mouse. At day 12, the mouse was sacrificed and CD4⁺ T cells from DLN, tumors, and non-DLN were analyzed.

BM chimeric mice. Six-week-old C57BL/6 female mice were injected i.p. for 3 days with 30 mg/kg busulfan. Mice were rescued by i.v. injection of 15×10^6 BM cells derived from C57BL/6 or from FcεRIγ-deficient mice. Chimeric mice were bred at a specific pathogen–free facility for 3 weeks prior to their challenge with B16F10 tumor cells.

Tumor immunotherapy. Animals were injected intratumorally with 80 μg anti-CD40 (clone FGK4.5; BioXCell) and 10 μg

TNF-α (BioLegend) and with or without 100 μg/mouse anti-human/mouse TRP1 IgG antibodies (clone TA99; BioXCell); 100 μg/mouse of anti-chicken ovalbumin (clone TOSGAA1; BioLegend) was used as control.

T cell isolation. All tissue preparations were performed simultaneously from each individual mouse (after euthanasia, by CO_2 inhalation). For isolation of T cells from lymphoid organs, the spleen, LN, and thymus were removed from euthanized mice and mashed through a 70 μM cell strainer (Gibco, Thermo Fisher Scientific). Cells were then washed by centrifugation at 800 *g* for 5 minutes at 4–8°C.

For isolation of tumor-infiltrating T cells, tumors were enzymatically digested with 2,000 U/ml of DNase I and 2 mg/mL collagenase IV (both from Sigma-Aldrich, Merck) in HBSS for 30 minutes at 37°C with a magnetic stirrer (400 rpm). Cells were then washed by centrifugation at 800 *g* for 5 minutes at 4–8°C.

T cells from PB. PB was collected via the posterior vena cava prior to perfusion of the animal and transferred into sodium heparin–coated vacuum tubes prior to 1:1 dilution in FACS buffer (HBSS, 2% FSC, 0.05 mM EDTA). Lymphocytes were enriched on a Ficoll-Paque Premium (Sigma-Aldrich) gradient, and collected PBMCs were washed twice with FACS buffer. For all tissues, cells were then incubated with anti-CD4 or anti-CD8 magnetic beads (MojoSort Nanobeads, BioLegend) according to the manufacturer's instructions and further sorted by FACSAriaII as $FCS^{lo}SSC^{lo}TCR\text{-}\beta^{+}MHC\text{-}II^{neg}$ cells.

T cell culture and expansion. T cells were cultured in RPMI-1640 supplemented with 1% penicillin-streptomycin, 10% heat-inactivated FBS, 1% sodium pyruvate, 1% MEM-Eagle nonessential amino acids, 1% insulin-transferrin-selenium, and 50 μM β-mercaptoethanol. For T cell expansion, culture dishes were precoated with 0.5 μg/mL anti-CD3 (clone 17A2) and 0.5 μg/mL anti-CD28 (clone 37.51) LEAF antibodies (both purchased from BioLegend) in PBS and were supplemented with 1,000 IU/mL recombinant murine IL-2 (PeproTech).

Mass spectrometry analysis. T cells were isolated as mentioned above and further sorted based on their FcγRI expression by FACSAriaIII into serum-free RPMI collection tubes. Cells were washed once with PBS, and the pellet was snap-frozen in liquid nitrogen and stored at –80°C. Samples were analyzed by The Smoler Proteomics Center at the Technion, Israel.

Lentiviral infection. For preparation of lentivirus, 1.3×10^6 HEK-293FT cells were plated on a 6-well plate precoated with 200 μg/mL poly-L-lysine and let to adhere overnight. pLVX plasmids containing wasabi under an EF1 promoter were mixed with psPAX2 (a gift from Didier Trono, Ecole Polytechnique Tédérale de Lausanne, Lausanne, Switzerland; Addgene plasmid 12260) and pCMV-VSV-G (a gift from Bob Weinberg, Massachusetts Institute of Technology, Cambridge, Massachusetts, USA; Addgene plasmid 8454) at a molar ratio of 3:2:1, and cells were transfected using Polyplus jetPRIME reagent (Polyplus Transfection). After 24 hours, medium was replaced with complete DMEM supplemented with 0.075% sodium bicarbonate. Medium-containing viruses were collected after 24 hours and 48 hours. For infection, virus-containing media were mixed with 100 μg/mL polybrene (Sigma-Aldrich) and added to B16 cells for 30 minutes at 37°C 5% CO_2. Cells were centrifuged for 30 minutes at 37°C and 450 *g*. Then, 80% of the medium was replaced with complete DMEM supplemented with 0.075% sodium bicarbonate. After 3 days in culture, cells that expressed wasabi were sorted by FACSAriaII, and cells were tested for mycoplasma, endotoxins, and bacterial contamination.

Retroviral infection. For retroviruses, Platinum E cells (a gift from Cyril Cohen, Tel Aviv University) were plated on 10 cm culture plates and cotransfected with a 2:1 molar ratio of pMIGII (46) and PCL-Eco plasmids (both were provided by Dario A.A. Vignali, University of Pittsburgh) using Polyplus jetPRIMEreagent (Polyplus Transfection). After 24 hours, the medium was replaced with complete DMEM supplemented with 0.075% sodium bicarbonate. Media-containing viruses were collected after 24 hours and 48 hours and centrifuged for 1 hour at 100,000 *g*. The pellet was resuspended gently in 1 mL media and let to recover overnight at 4°C. Prior to infection, splenic $CD4^+$ T cells were incubated on a plate precoated with anti-CD3 (0.5 μg/mL) in T cell medium containing high-dose IL-2 (1,000 IU/ml). Next, 0.3 mL concentrated retroviruses was added to every group of 2×10^6 $CD4^+$ T cells with 10 μg/mL polybrene. Cells were incubated for 30 minutes at 37°C in 5% CO_2 and centrifuged at 37°C, 800 *g*, for 1 hour. Afterwards, 80% of medium was replaced and T cells were cultured for an additional 3 days in T cell media containing high-dose IL-2.

Adoptive T cell transfer. C57BL/6 mice were injected s.c. with 2×10^5 B16F10 tumor cells. On days 12 and 14, mice were injected intratumorally with 80 μg anti-CD40 (clone FGK4.5; BioXCell) and 1 μg IFN-γ (BioLegend) and 200 μg anti-TRP1. On day 7, mice were euthanized and the tumors and DLNs were removed and dissociated to obtain single-cell suspension. T cells were then enriched on magnetic beads (EasySep, STEMCELL Technologies) and further sorted by FACSAriaII as $FCS^{lo}SSC^{lo}TCR\text{-}\beta^{+}MHC\text{-}II^{neg}$ cells. T cells were cultured in T cell medium containing 1,000 IU/mL IL-2 (Peprotech) on culture plates coated with 0.5 μg/mL of anti-CD3. After 9–12 days, T cells were gently collected and a total of 1×10^6 cells was injected intravenously into mice bearing tumors with an average size of 30–50 mm^2.

Immunohistochemistry. For frozen sections, mouse and human tissues were fixed in 4% paraformaldehyde for 1 hour and equilibrated in a 20% sucrose solution overnight. Tissues were then embedded in frozen tissue matrix (Scigen O.C.T. Compound Cryostat Embedding Medium, Thermo Fisher Scientific) and frozen at –80°C. The 5 μm thick sections were blocked with 5% BSA and stained with 1:100 diluted primary antibodies. For anti-mouse staining, we used anti-CD3 (clone 17A2), anti-CD4 (clone RM4-4), anti–TCR-β (clone H57-597), anti-FcRI (clone X54-5/7.1), anti-FcRII/III (clone 93), and anti-FcRIV (clone 9E9); for the human panel, we used anti-CD3(clone HIT3a), anti-CD4 (clone RPA-T4), anti-CD8 (clone HIT8a), anti-CD16 (clone 3G8), and anti-CD32 (clone FUN-2), all from BioLegend. Nuclei were counterstained with Hoechst 33342 (Fluka). Microscopy was performed with a Zeiss LSM 800 confocal microscope and analyzed using ZEN software (ZEISS).

Confocal microscopy. B16-Wasabi and $CD4^+$ T cells were cocultured on glass-bottom confocal plates (Cellvis) in T cell medium without IL-2 and incubated overnight under standard conditions. Cells were further incubated for 1 hour with BV421-conjugated anti-CD107 (BioLegend) at a 1:100 dilution. Images were collected using a Zeiss LSM800 confocal laser scanning microscope and analyzed using ZEN software (ZEISS).

Killing assay. $CD4^+$ T cells were cocultured with B16 target cells (30,000 cells per well) at a ratio of 1:2 (T:E) in a round-bottom 96-well plate with or without the following antibodies: anti-chicken ovalbumin (clone TOSGAA1; BioLegend), anti–TRP-1 (clone TA99; BioXCell), or anti–TRP-1 $F(ab')_2$. After 24 hours and 48 hours, the medium was

replaced with PBS, and the fluorescence intensity of wasabi (excitation, 485 nm; emission, 528 nm) was measured by a Synergy H1M plate reader (BioTek). After 48 hours, cells were stained with annexin V (BioLegend) for 15 minutes and propidium iodide (PI) for 2 minutes on ice, and staining levels were analyzed by flow cytometry.

Preparation of F(ab′)$_2$ fragment. Anti-TRP1 antibody (clone TA99; BioXCell) was dialyzed against 20 mm sodium acetate pH 4.5 and digested with agarose-pepsin beads (GoldBio) for 16 hours in a 37°C incubator with rotation. Next, the sample was centrifuged and supernatant was collected, dialyzed against PBS pH 7.4, and incubated with protein-A agarose beads (Santa Cruz Biotechnology) for 2 hours with rotation. The F(ab′)$_2$ fraction was collected after centrifugation and was analyzed by PAGE.

Flow cytometry. Purified T cells were analyzed using flow cytometry (CytoFLEX, Beckman Coulter) and sorted by FACS (BD FACSAria III, BD Biosciences). Data sets were analyzed using FlowJo software (Tree Star). mAbs for anti-TRP1 conjugated to FITC or specific for the following mouse antigens were used: Alexa Fluor 647 or Brilliant Violet 421, CD3 (clone 17A2); phycoerythrin, CD4 (clone RM 4-4); Brilliant Violet 605, CD8 (clone 53-6.7); Alexa Fluor 488, CD11b (clone M1/70); APC/Cy7, CD44 (clone IM7); phycoerythrin /Cy7, CD62L (clone MEL-14); Alexa Fluor 647, FcRIV (clone 9E9); Brilliant Violet 421, TCRb (clone H57-597); allophycocyanin, MHC-II (clone M5/114.15.2); fluorescein, FcRI (clone X54-5/7.1); and phycoerythrin/Cy7, FcRII/III (clone 93). For humans, the following specific antigens were used: Alexa Fluor 488, CD3 (clone HIT3a); Alexa Fluor 594, CD4 (clone RPA-T4); allophycocyanin, CD19 (clone HIB19); Alexa Fluor 647, CD8 (clone HIT8a), Brilliant Violet 650, CD11c (clone 3.9); Alexa Fluor 647, CD16 (clone 3G8); PerCp/Cy5.5, CD32 (clone FUN-2); Brilliant Violet 421, CD64 (clone 10.1); allophycocyanin/Cy7, CD45RO (clone UCHL1); phycoerythrin/Cy7, CD45RA (clone HI100). All Abs were purchased from BioLegend. Cells were suspended in FACS buffer consisting of HBSS with 2% FCS and 0.05 mM EDTA.

TCR repertoire analysis. FcγRI$^+$ and FcγRI^{neg}CD4$^+$ T cells were sorted from the spleens of naive C57BL/6 male mice. Total RNA was immediately extracted from sorted cells using the RNeasy Micro Kit (QIAGEN). Amplification of TCR-α and -β chain cDNA was performed using a SMARTer Mouse TCR α/β Profiling Kit (Takara Bio Inc.) according to the manufacturer's protocol. Resultant cDNA libraries were sequenced by Illumina MiSeq 250x2 (Kit v2) by HyLabs Ltd., and data were analyzed with VDJServer (https://vdjserver.org/project).

PCR amplification of CD3 and FcγRI. Total RNA was purified from CD11b$^+$, FcγRI$^+$, and FcγRI^{neg}CD4$^+$ sorted cells using the RNeasy Micro Kit (QIAGEN) and was quantified using NanoDrop One (Thermo Fisher Scientific). Reverse transcription was performed using a qScript cDNA Synthesis Kit (Quanta Biosciences) according to the manufacturer's protocol. cDNA samples were analyzed by PCR for the detection of the FcγRI sequence using AGACACCGCTACACATCTGC and GGGAAGTTTGTGCCCCAGTA primers and the CD3ε polypeptide sequence using GCATTCTGAGAGGATGCGGT and TGGCCTTGGCCTTCCTATTC primers. These were analyzed by agarose gel electrophoresis.

Statistics. Each experiment was performed 3 times. Each experimental group consisted of at least 3 mice. Significance of results was determined using nonparametric 1-way ANOVA when multiple groups were analyzed with Tukey's post test. For multiple parameters analysis, 2-way ANOVA was performed with Bonferroni-Šidák post test. For 2-group analysis, 1-way ANOVA with Dunn's test was performed. For time course data and growth curves, *P* values were calculated by 2-way ANOVA with Tukey's post test.

Study approval. All mice were housed in an animal facility accredited by the American Association for the Accreditation of Laboratory Animal Care and were maintained under specific pathogen–free conditions. Animal experiments were approved and conducted in accordance with Tel Aviv University Laboratory Accreditation (01-16-095). The Tel Aviv University Institutional Review Board approved the human subject protocols, and informed consent was obtained from all subjects prior to participation in the study.

Author contributions

DR and NSM conducted the majority of the experiments and helped to design them. LT, AG, and LFY conducted some of the experiments. CS helped with generating the FcγRI constructs and writing the manuscript. NRF made the viral vectors for labeling the tumor cells and has helped with writing the manuscript. YW helped with analyzing the TCR sequencing data. HG, AT, and RB provided biological materials from human cancer patients. EAB assisted with the acquisition of human samples to use for experimentation. PR and YC designed and conducted the experiments and wrote the manuscript.

Acknowledgments

This work was funded by The Swiss Bridge Foundation, the Israel Cancer Association (grant number 20180041), and the Israel Science Foundation (ISF) (grant number 2262/18). The authors would like to deeply thank Edgar G. Engleman from Stanford University, Gidi Gross from the Migal Research Institute, and Adi Barzel from Tel Aviv University for their insightful comments and helpful discussions. We would also like to thank Tomer Meir Salame from the Weizmann Institute for his help with flow cytometry.

Address correspondence to: Yaron Carmi, Department of Pathology, Sackler School of Medicine, Tel Aviv University, Tel Aviv 69978, Israel. Phone: 972.36409504; Email: yaron.carmi@gmail.com.

1. Coussens LM, Zitvogel L, Palucka AK. Neutralizing tumor-promoting chronic inflammation: a magic bullet? *Science*. 2013;339(6117):286–291.
2. Hanahan D, Coussens LM. Accessories to the crime: functions of cells recruited to the tumor microenvironment. *Cancer Cell*. 2012;21(3):309–322.
3. Bindea G, et al. Spatiotemporal dynamics of intratumoral immune cells reveal the immune landscape in human cancer. *Immunity*. 2013;39(4):782–795.
4. Pagès F, Galon J, Dieu-Nosjean MC, Tartour E, Sautès-Fridman C, Fridman WH. Immune infiltration in human tumors: a prognostic factor that should not be ignored. *Oncogene*. 2010;29(8):1093–1102.
5. Tsou P, Katayama H, Ostrin EJ, Hanash SM. The Emerging Role of B Cells in Tumor Immunity. *Cancer Res*. 2016;76(19):5597–5601.
6. Yuen GJ, Demissie E, Pillai S. B lymphocytes and cancer: a love-hate relationship. *Trends Cancer*. 2016;2(12):747–757.
7. Qin Z, Richter G, Schüler T, Ibe S, Cao X, Blankenstein T. B cells inhibit induction of T cell-dependent tumor immunity. *Nat Med*. 1998;4(5):627–630.
8. Inoue S, Leitner WW, Golding B, Scott D. Inhibitory effects of B cells on antitumor immunity. *Cancer Res*. 2006;66(15):7741–7747.
9. Bodogai M, et al. Anti-CD20 antibody promotes

cancer escape via enrichment of tumor-evoked regulatory B cells expressing low levels of CD20 and CD137L. *Cancer Res*. 2013;73(7):2127–2138.
10. Willimsky G, et al. Immunogenicity of premalignant lesions is the primary cause of general cytotoxic T lymphocyte unresponsiveness. *J Exp Med*. 2008;205(7):1687–1700.
11. Georgoudaki AM, et al. Reprogramming tumor-associated macrophages by antibody targeting inhibits cancer progression and metastasis. *Cell Rep*. 2016;15(9):2000–2011.
12. Somasundaram R, et al. Tumor-associated B-cells induce tumor heterogeneity and therapy resistance. *Nat Commun*. 2017;8(1):607.
13. de Visser KE, Korets LV, Coussens LM. De novo carcinogenesis promoted by chronic inflammation is B lymphocyte dependent. *Cancer Cell*. 2005;7(5):411–423.
14. Yang C, et al. B cells promote tumor progression via STAT3 regulated-angiogenesis. *PLoS ONE*. 2013;8(5):e64159.
15. Nimmerjahn F, Ravetch JV. Divergent immunoglobulin g subclass activity through selective Fc receptor binding. *Science*. 2005;310(5753):1510–1512.
16. Carmi Y, et al. Akt and SHP-1 are DC-intrinsic checkpoints for tumor immunity. *JCI Insight*. 2016;1(18):e89020.
17. DiLillo DJ, Ravetch JV. Differential Fc-receptor engagement drives an anti-tumor vaccinal effect. *Cell*. 2015;161(5):1035–1045.
18. Zhu EF, et al. Synergistic innate and adaptive immune response to combination immunotherapy with anti-tumor antigen antibodies and extended serum half-life IL-2. *Cancer Cell*. 2015;27(4):489–501.
19. DiLillo DJ, Yanaba K, Tedder TF. B cells are required for optimal CD4+ and CD8+ T cell tumor immunity: therapeutic B cell depletion enhances B16 melanoma growth in mice. *J Immunol*. 2010;184(7):4006–4016.
20. Li Q, et al. Adoptive transfer of tumor reactive B cells confers host T-cell immunity and tumor regression. *Clin Cancer Res*. 2011;17(15):4987–4995.
21. Scott AM, Allison JP, Wolchok JD. Monoclonal antibodies in cancer therapy. *Cancer Immun*. 2012;12:14.
22. Reuschenbach M, von Knebel Doeberitz M, Wentzensen N. A systematic review of humoral immune responses against tumor antigens. *Cancer Immunol Immunother*. 2009;58(10):1535–1544.
23. Fridman WH, Pagès F, Sautès-Fridman C, Galon J. The immune contexture in human tumours: impact on clinical outcome. *Nat Rev Cancer*. 2012;12(4):298–306.
24. Tang Y, Lou J, Alpaugh RK, Robinson MK, Marks JD, Weiner LM. Regulation of antibody-dependent cellular cytotoxicity by IgG intrinsic and apparent affinity for target antigen. *J Immunol*. 2007;179(5):2815–2823.
25. Rudnick SI, Adams GP. Affinity and avidity in antibody-based tumor targeting. *Cancer Biother Radiopharm*. 2009;24(2):155–161.
26. Kaneko Y, Nimmerjahn F, Ravetch JV. Anti-inflammatory activity of immunoglobulin G resulting from Fc sialylation. *Science*. 2006;313(5787):670–673.
27. Li T, DiLillo DJ, Bournazos S, Giddens JP, Ravetch JV, Wang LX. Modulating IgG effector function by Fc glycan engineering. *Proc Natl Acad Sci U S A*. 2017;114(13):3485–3490.
28. Carmi Y, et al. Allogeneic IgG combined with dendritic cell stimuli induce antitumour T-cell immunity. *Nature*. 2015;521(7550):99–104.
29. Rosales C. Fcγ Receptor Heterogeneity in Leukocyte Functional Responses. *Front Immunol*. 2017;8:280.
30. Shah S, et al. Increased rejection of primary tumors in mice lacking B cells: inhibition of anti-tumor CTL and TH1 cytokine responses by B cells. *Int J Cancer*. 2005;117(4):574–586.
31. Chauhan AK. Human CD4(+) T-cells: a role for low-affinity Fc receptors. *Front Immunol*. 2016;7:215.
32. Nimmerjahn F, Ravetch JV. Fcgamma receptors as regulators of immune responses. *Nat Rev Immunol*. 2008;8(1):34–47.
33. Chauhan AK, Chen C, Moore TL, DiPaolo RJ. Induced expression of FcγRIIIa (CD16a) on CD4+ T cells triggers generation of IFN-γhigh subset. *J Biol Chem*. 2015;290(8):5127–5140.
34. Thorsson V, et al. The immune landscape of cancer. *Immunity*. 2018;48(4):812–830.e14.
35. Bevan MJ. Helping the CD8(+) T-cell response. *Nat Rev Immunol*. 2004;4(8):595–602.
36. Castellino F, Germain RN. Cooperation between CD4+ and CD8+ T cells: when, where, and how. *Annu Rev Immunol*. 2006;24:519–540.
37. Ahrends T, et al. CD4$^+$ T cell help confers a cytotoxic T cell effector program including coinhibitory receptor downregulation and increased tissue invasiveness. *Immunity*. 2017;47(5):848–861.e5.
38. Shedlock DJ, Shen H. Requirement for CD4 T cell help in generating functional CD8 T cell memory. *Science*. 2003;300(5617):337–339.
39. Janssen EM, Lemmens EE, Wolfe T, Christen U, von Herrath MG, Schoenberger SP. CD4+ T cells are required for secondary expansion and memory in CD8+ T lymphocytes. *Nature*. 2003;421(6925):852–856.
40. Hunder NN, et al. Treatment of metastatic melanoma with autologous CD4+ T cells against NY-ESO-1. *N Engl J Med*. 2008;358(25):2698–2703.
41. Tran E, et al. Cancer immunotherapy based on mutation-specific CD4+ T cells in a patient with epithelial cancer. *Science*. 2014;344(6184):641–645.
42. Muranski P, et al. Tumor-specific Th17-polarized cells eradicate large established melanoma. *Blood*. 2008;112(2):362–373.
43. Xie Y, et al. Naive tumor-specific CD4(+) T cells differentiated in vivo eradicate established melanoma. *J Exp Med*. 2010;207(3):651–667.
44. Quezada SA, et al. Tumor-reactive CD4(+) T cells develop cytotoxic activity and eradicate large established melanoma after transfer into lymphopenic hosts. *J Exp Med*. 2010;207(3):637–650.
45. Matsuzaki J, et al. Direct tumor recognition by a human CD4(+) T-cell subset potently mediates tumor growth inhibition and orchestrates anti-tumor immune responses. *Sci Rep*. 2015;5:14896.
46. Bettini ML, Bettini M, Nakayama M, Guy CS, Vignali DA. Generation of T cell receptor-retrogenic mice: improved retroviral-mediated stem cell gene transfer. *Nat Protoc*. 2013;8(10):1837–1840.